Cirrus Induced Polarization in 122 GHz Aura Microwave Limb Sounder Radiances

C. P. Davis,[1] D. L. Wu,[2] C. Emde,[3] J. H. Jiang,[2] R. E. Cofield,[2] and R. S. Harwood[1]

Previous simulation studies have outlined the possibility of significant polarization signals in microwave limb sounding due to horizontally aligned ice crystals in cirrus clouds. From the recently launched Aura MLS instrument, we present the first polarized microwave limb sounding observations of cirrus clouds. We also present polarized radiative transfer simulations, which show good qualitative agreement with these observations, and indicate the limits to which aligned non-spherical particles are influencing bulk optical properties of cirrus clouds at microwave wavelengths. Although 122 GHz is not ideal for cloud measurements due to strong O_2 absorption, data and simulations indicate that preferential crystal orientation is causing small, but noticeable, partial vertical polarization, which can be replicated in simulations by considering all particles as horizontally aligned oblate spheroids with aspect ratios of around 1.2 $\pm$ 0.15.

1. Introduction

The EOS Aura Microwave Limb Sounder (MLS) has been fully operational since 13 August 2004. Aura MLS makes daily global measurements of stratospheric temperature, geopotential height, water vapour, O_3, OH, HO_2, CO, HCN, CH_3CN, N_2O, HNO_3, HCl, HOCl, ClO, BrO, and volcanic SO_2. Several of these measurements are also made in the mid- to upper-troposphere (e.g. 12 [@]). Ice clouds can adversely affect these tropospheric measurements. On the other hand, the effect of cirrus on received radiances can provide information on cloud properties; indeed, ice water content (IWC) has been included as a MLS data product.

A thorough treatment of the effect of cirrus on MLS measurements requires the consideration of polarization. Czekala 6 [@] showed that of all possible viewing geometries, limb sounding would be most affected by cloud induced polarization where there are non-spherical preferentially aligned ice crystals. Miao 16 [@] studied the utilization of cirrus induced polarization in a possible slant viewing mm/sub-mm cloud sensor. To investigate the polarization effect on Aura MLS, a 3D polarized forward model was developed 8 [@], and incorporated into the freely available ARTS software package (http://www.sat.uni-bremen.de/arts).

[1]Institute of Atmospheric and Environmental Science, University of Edinburgh, Edinburgh, UK

[2]Jet Propulsion Laboratory, California Institute of Technology, Pasadena

[3]Institute for Envronmental Physics, University of Bremen, Bremen, Germany

0094-8276/05/$5.00

Refs. 6 [@], 16 [@], 8 [@], and 10 [@], have all shown that the orientation distribution is the dominant factor in determining the magnitude of the polarization signal. However, the extent to which preferentially aligned non-spherical particles affect the bulk optical properties of cirrus clouds at microwave frequencies is unknown. It is well known that falling plate and column crystals have a preferred horizontal orientation, but in cirrus clouds pristine crystals (plates,columns) are generally outnumbered by aggregates (e.g 2 [@]), which have an infinite variety of complex shapes, and whose orientation behaviour is unclear. The presence of large randomly oriented particles will strongly dilute the polarizing influence of horizontally aligned pristine crystals. Using a ice crystal aggregation model Westbrook et. al. 26 [@] showed that as aggregates grew, they asymptotically approached an aspect ratio of 0.65$\pm$ 0.05, which agreed well with in situ observations. It seems reasonable to postulate that such aggregate particles may have a preferred orientation with the longest dimension parallel to the horizontal, but that the orientation distribution will be broader than that of pristine particles. Measurements of solar reflectance by the POLDER/ADEOS instrument 4 [@] indicated that horizontal ice crystal alignment was noticeable in 40% of cirrus observations.

Space-borne off-nadir polarized mm/sub-mm observations of cirrus will help establish whether preferentially oriented ice crystals substantially affect the bulk optical properties of cirrus clouds. In turn, this information may impact on any future plans for any polarization based cirrus measurements (e.g. 16 [@]), and will help evaluate whether the computational expense of polarized radiative transfer is justified in retrieval software for space-borne off-nadir microwave instruments. In this paper we present the first such observations.

The EOS-MLS instrument is on board the Aura spacecraft, which was successfully launched on 15 July 2004. The MLS instrument incorporates five radiometers with broad bands centred at 118 GHz, 190 GHz, 240 GHz, 640 GHz, and 2.5 THz, labelled R1 to R5 respectively. For cloud detection it is preferable to use window channels, where atmospheric absorption and emission is relatively weak. This gives cloud affected radiances the greatest contrast with those for clear-sky cases. In the case of low tangent heights, where the received radiation emanates from the lower troposphere in clear cases, clouds produce a significant brightness temperature depression (negative ΔT_b), and for high tangent heights, where the background is cold in clear sky cases, we can get a significant brightness temperature enhancement. Example window frequencies for Aura MLS are 200.5 GHz in R2, and 230 GHz in R3. However, in this study we use radiances from R1, because for this frequency range we are able to obtain both horizontally and vertically polarized components of the limb radiation. R1A, and R1B have orthogonal antenna polarizations, V and H respectively, where the V axis corresponds to the direction that is perpendicular to the direction of propagation and lying on the plane containing the propagation direction and the local zenith. For this study we choose data from channel 1 of band 32 (R1A), and band 34(R1B), which are single 0.5 GHz wide filters centred

at 122 GHz. This channel is the furthest from the 118 GHz O_2 line, and therefore the most sensitive to cloud. Although this channel is not as sensitive to cirrus as some of those in R2 and R3, high thick cirrus can cause brightness temperature depressions as large as $\Delta T_b = -50$ K for low tangent heights.

In this paper, these channels are used to calculate the total radiance, $I = I_v + I_h$, and the polarization difference, $Q = I_v - I_h$, which characterises the degree of horizontal or vertical polarization. Polarized radiative transfer simulations are are presented to help interpret the observed polarization data. Specifically, the ARTS-DOIT 1D discrete ordinates model 10 [@] is used to give simulated Stokes vectors for various thin-layer cirrus scenarios, while the 3D ARTS-MC reversed Monte Carlo model 8 [@] is used to give simulated Stokes vectors for various horizontally confined deep cirrus scenarios representing tropical convective cirrus.

2. Polarized MLS RT simulations for 122 GHz

The intensity and polarization state of a beam of incoherent electromagnetic radiation is described by the Stokes' vector $\mathbf{I} = [I, Q, U, V]^T$. Here we express these parameters as Rayleigh Jeans brightness temperatures. Simulation of the Stokes vector for a given propagation direction $\mathbf{n}$ at the MLS antenna is achieved by solving the vector radiative transfer equation (VRTE) (e.g. 20 [@]):

$$\frac{d\mathbf{I}(\mathbf{n})}{ds} = -\mathbf{K}(\mathbf{n})\mathbf{I}(\mathbf{n}) + \mathbf{K_a}(\mathbf{n})I_b(T) + \int_{4\pi} \mathbf{Z}(\mathbf{n},\mathbf{n}')\mathbf{I}(\mathbf{n}')d\mathbf{n}' \quad (1)$$

s is distance along direction $\mathbf{n}$ and I_b is the Planck radiance. $\mathbf{K}(\mathbf{n})$, $\mathbf{K_a}(\mathbf{n})$, and $\mathbf{Z}(\mathbf{n},\mathbf{n}')$ are the bulk extinction matrix, absorption coefficient vector and phase matrix of the medium respectively. For brevity these have been expressed as bulk optical properties, where individual single scattering properties have been multiplied by particle number density and summed over all orientations and particle types. The argument $\mathbf{n}$ has been retained to signify that in general these properties depend on the direction of propagation.

In this study two algorithms are used for the solution of the VRTE, both of which belong to the ARTS software package (http://www.sat.uni-bremen.de/arts). ARTS-DOIT 10 [@] is an iterative discrete ordinates type radiative transfer model, which calculates the Stokes vector for an array of directions at every grid point in the scattering domain. ARTS-MC, which emplys a reversed Monte Carlo RT algorithm 8 [@], calculates the Stokes vector only for the desired sensor position and viewing direction. For 3D simulations ARTS-MC is generally preferred for its reduced CPU and memory requirements. Crucial to the suitability of the ARTS platform for limb sounding simulations is its incorporation of 3D spherical geometry.

In the following simulations two cloud types are considered: a thin cirrus scenario with a cloud base at 11.9 km and a cloud top at 13.4 km; and a deep cirrus scenario with a base at 6km, a top at 16km, and a horizontal extent of 50km in zonal and meridional directions. For the thin-layer case ARTS-DOIT is used in 1D mode, and for the deep cirrus case ARTS-MC is used. A single representative tropical profile is used for temperature and water vapour fields. Particle size distributions are obtained from ice water content (IWC) and temperature fields using the McFarquhar and Heymsfield 14 [@] size distribution for tropical cirrus. Single scattering properties for horizontally aligned non-spherical particles (spheroids or cylinders) are calculated using the PyARTS python package (http://www.met.ed.ac.uk/~cory/PyARTS), which combines the T-matrix code of Mishchenko 18 [@], and the ice refractive index data of Warren 24 [@], to give $\mathbf{K}(\mathbf{n})$, $\mathbf{K_a}(\mathbf{n})$, and $\mathbf{Z}(\mathbf{n},\mathbf{n}')$ in an ARTS readable format.

The expected polarization behaviour of cirrus affected 122 GHz MLS radiances is demonstrated in Fig. 1, which shows example 122 GHz radiative transfer simulations for the 3D deep cirrus scenario described above. Five different particle shape/orientation combinations were used: horizontally aligned prolate spheroids with aspect ratio 0.5, spheres, horizontally aligned oblate spheroids with aspect ratio 2.0, randomly aligned prolate cylinders with aspect ratio 0.5, and horizontally aligned prolate spheroids with aspect ratio 0.5. For the prolate particles, their axis of rotation is orientated randomly with respect to the azimuth. In each case, the cloud had a uniform IWC of 0.2 gm^{-3}. In these simulations the field of view characteristics of the Aura MLS antenna have not been explicitly considered; they consider only a pencil-beam.

The first panel in Fig. 1 indicates that the choice of particle type and orientation scheme has only a small relative effect on the total radiance. However, particle type, and orientation does have a significant impact on the polarization difference. Although randomly oriented prolate cylinders behave almost exactly like spherical particles (of the same volume), the horizontally aligned non-spherical particles give significant partial vertical polarization for low tangent heights. Fig. 1 suggests that for very high clouds, and for tangent heights nearing 16km, we could see small positive values for ΔI_{cir}, and that in these cases there will be slight horizontal polarization for horizontally aligned particles. However, the rapid variation with tangent height makes these high tangent height predictions sensitive to field of view averaging.

The sign of the polarization signal is determined by the magnitude of two opposing mechanisms: dichroism, which is the effect of a non-diagonal extinction matrix, $\mathbf{K}$; and the effect of radiation being scattered into the line of sight, which

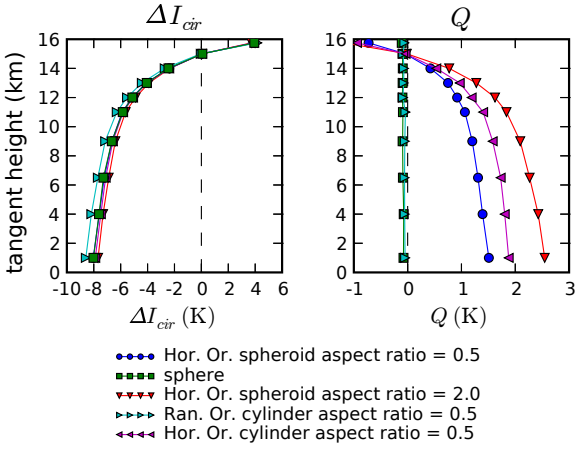

Figure 1. Example 122 GHz radiative transfer simulations for the 3D deep cirrus scenario with different shape/orientation combinations. In each case, the cloud has a uniform IWC of 0.2 gm^{-3}.

is described by the last term in Eq. 1. In the cases presented here the horizontally aligned non-spherical particles have a negative K_{21}, which has the effect of vertically polarizing radiation. The magnitude of this effect on the measured radiance depends on the source radiance. The contribution to the polarization signal of radiation scattered into the line of sight depends on both the spatial distribution of incoming radiance, and the shape and orientation of scattering particles, which, in the case of horizontally aligned particles, contributes to horizontal polarization. The mechanisms above combine to give the variation in Q with tangent height. For high tangent heights the radiative background is cold so that the dichroism effect is smaller in comparison with the scattering integral contribution. This yields the lower Q at high tangent heights. The warmer source radiance at low tangent heights increases the dichroism effect - giving positive Q.

Fig. 1 indicates that the ΔI_{cir} and Q profiles for all of the considered shape/orientation combinations can be well reproduced by choosing an oblate or prolate spheroid with an appropriate aspect ratio. Although cirrus contain a variety of crystal shapes, with an unknown degree of horizontal alignment, for the purpose of this study we will assume that MLS ΔI_{cir} and Q profiles for real cirrus can also be adequately reproduced by horizontally aligned spheroids (prolate or oblate) with an appropriately chosen aspect ratio.

3. Example Aura MLS Observations of Q for 122 GHz

ΔI_{cir} and Q can be obtained from Aura MLS level 1B (L1B) radiance files. A daily L1B file contains data for 14 orbits which is comprised of approximately 3495 limb scans, or major frames (MAFs), which in turn contain 125 minor frames (MIFs). Some steps are needed to refine the R1A and R1B radiometric calibration for accurate Q calculation. Firstly, any bias in the R1A-R1B space-view radiances are removed by subtracting the mean of brightness temperatures for tangent heights greater than 50 km. Secondly we apply a 3.5% gain correction to the R1B radiances for MLS L1B versions 1.5 and older. After making these corrections to T_b^{R1A} and T_b^{R1B}, I and Q are given by $0.5\left(T_b^{\mathrm{R1A}}+T_b^{\mathrm{R1B}}\right)$ and $0.5\left(T_b^{\mathrm{R1A}}-T_b^{\mathrm{R1B}}\right)$ respectively. Finally, to calculate the cloud induced radiance, ΔI_{cir}, we pass I values for all the MAFs for each tangent height through a high pass filter with a window width of 19 MAFS along the orbit track.

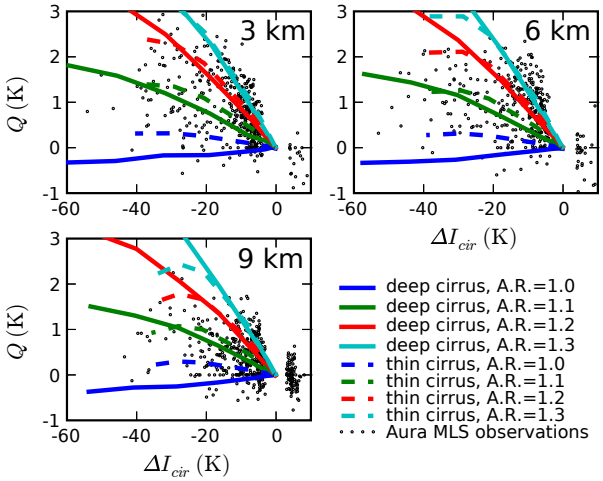

Figure 3. Observed and simulated Q vs. ΔI_{cir}.

In this way we use the temporal variation in radiance to detect cloud events. Q is also high pass filtered to remove remaining second order effects related to the R1A/R1B gain mismatch.

In Fig. 2 ΔI_{cir} and Q are shown for 3 - 8 January 2005. Fig. 2 shows a high frequency of cloud affected radiances in a region centred slightly south of the equator. This can be be explained by the inability of R1 to detect low clouds, and the prevalence of high ice clouds due to the position of the inter-tropical convergence zone and the region of increased tropopause height, which are consistent with the northern hemisphere winter. Clear sky variance has been screened from the ΔI_{cir} in Fig. 2 by only including points that differ from zero by more than 2σ. In the second row of Fig. 2 we see a region with observations of partial vertical polarization (positive Q) coinciding with the latitude range of cloud induced ΔI_{cir}. The variation in ΔI_{cir} and Q with tangent height are in good qualitative agreement with the example RT simulations shown in Fig. 1.

In Fig. 3 the association of the partial vertical polarization with clouds is clarified by plotting Q against ΔI_{cir}. Only cloudy points, where $|\Delta I_{cir}| > 2\sigma$, are shown. We see that a majority of the cloudy points have positive Q values, indicating partial vertical polarization. The period of January 3-8 was chosen for its relative lack of disturbances due to spacecraft operations and other anomalies. In every other respect the behaviour shown in Figs. in 2 and 3 is typical for all days to date, except for the meridional distribution of cloud events, which varies seasonally.

Also shown in Fig. 3 are simulated Q vs. ΔI_{cir} curves for horizontally aligned oblate spheroids with aspect ratios 1.0(spheres), 1.1, 1.2 and 1.3. Each curve represents a range of IWC from 0.01 gm^{-3}, which has negligible effect on the simulated Stokes vector, to 1 gm^{-3}. Curves are shown for both the deep (solid) and thin (dashed) cirrus scenarios described above.

Most data points lie between the simulation curves for aspect ratios 1.1 and 1.3, which indicates that the bulk extinction matrix is noticeably non-diagonal, indicating an influence from oriented particles. The spread of the clear-sky Q values in Fig. 2 indicates a low signal to noise ratio for the cloud induced polarization. However, from these results it seems reasonable to conclude that the Stokes vector for cloud affected 122 GHz MLS measurements can be adequately reproduced by considering all hydrometeors as horizontally aligned oblate spheroids with aspect ratio 1.2 $\pm$ 0.15.

4. Conclusion

Because of strong gaseous absorption, 122 GHz is not particularly sensitive to clouds, yet these observations show a noticeable cirrus induced polarization. For window channels this signal will be larger. Q values become particularly interesting for window frequencies in R2 and R3, because these radiometers have orthogonal polarizations, V and H respectively.

The results presented here for 122 GHz suggest the possibility of retrieving cirrus particle shape/orientation information. Cirrus crystal shape and orientation have a significant importance when considering the impact of cirrus on the earth's radiation budget (e.g. 22 [@]). The retrieval of cirrus particle shape and orientation information from Aura MLS R1, R2, and R3 data is a topic for further study.

Acknowledgments. The authors wish to thank the entire Aura MLS team and the developers of the ARTS software package. Thanks are also due to Michael Mishchenko and Stephen Warren for the availability of the T-matrix and ice refractive index

codes respectively. Cory Davis is funded by the National Environment Research Council (UK) under the Clouds Water Vapour and Climate thematic programme.

References

A.J. Baran. On the scatting and absorption properties of cirrus cloud. *Journal of Quantitative Spectroscopy and Radiative Transfer*, 89:17–36, 2004.

H. Chepfer, G. Brogniez, P. Goloub, F. Breon, and P. Flamant. Observations of horizontally oriented ice crystals in cirrus clouds with polder-1/adeos-1. *J. Quant. Spectros. Rad. Trans*, 63:521–543, 1999.

H. Czekala. Effects of ice particle shape and orientation on polarized microwave radiation for off nadir problems. *Geophys. Res. Lett.*, 25(10):1669–1672, 1998.

C. Davis, C. Emde, and R. Harwood. A 3D polarized reversed monte carlo radiative transfer model for mm and sub-mm passive remote sensing in cloudy atmospheres. *IEEE Trans. Geosci. Remote Sensing*, page in press, 2005.

C. Emde, S. A. Buehler, C. Davis, P. Eriksson, T. R. Sreerekha, and C. Teichmann. A polarized discrete ordinate scattering model for simulations of limb and nadir longwave measurements in 1d/3d spherical atmospheres. *J. Geophys. Res.*, 109(D24207), 2004. doi:10.1029/2004JD005140.

J.W. Waters et. al. The UARS and EOS microwave limb sounder (MLS) experiments. *Journal of the Atmospheric Sciences*, 56:194–218, 1999.

G.M. McFarquhar and A.J. Heymsfield. Parametrization of tropical ice crystal size distributions and implications for radiative transfer: Results from cepex. *J. Atmos. Sci.*, 54:2187–2200, 1997.

J. Miao, K.-P. Johnson, S. Buehler, and A. Kokhanovsky. The potential of polarization measurements from space at mm and sub-mm wavelengths for determining cirrus cloud parameters. *Atmos. Chem. Phys.*, 3:39–48, 2003.

M.I. Mishchenko. Calculation of the amplitude matrix for a nonspherical particle in a fixed orientation. *Applied Optics*, 39(6):1026–1031, 2000.

M.I. Mishchenko, J.W. Hovenier, and L.D. Travis. *Light Scattering by Non-spherical Particles.* Academic Press, 2000.

Y. Takano and K.-N. Liou. Solar radiative transfer in cirrus clouds. part ii: Theory and computation of multiple scattering in an anisotropic medium. *Journal of the Atmospheric Sciences*, 46(1):20–46, 1989.

S.G. Warren. Optical constants of ice from the ultraviolet to the microwave. *Applied Optics*, 23(8):1206–1225, 1984.

C.D. Westbrook, R. C. Ball, P.R. Field, and A. Heymsfield. A theory of growth by differential sedimentation, with application to snowflake formation. *Phys. Rev. E*, 70(021403), 2004.

C. P. Davis, Institute of Atmospheric and Environmental Science, University of Edinburgh, EH92NN, UK. (cdavis@staffmailed.ac.uk)

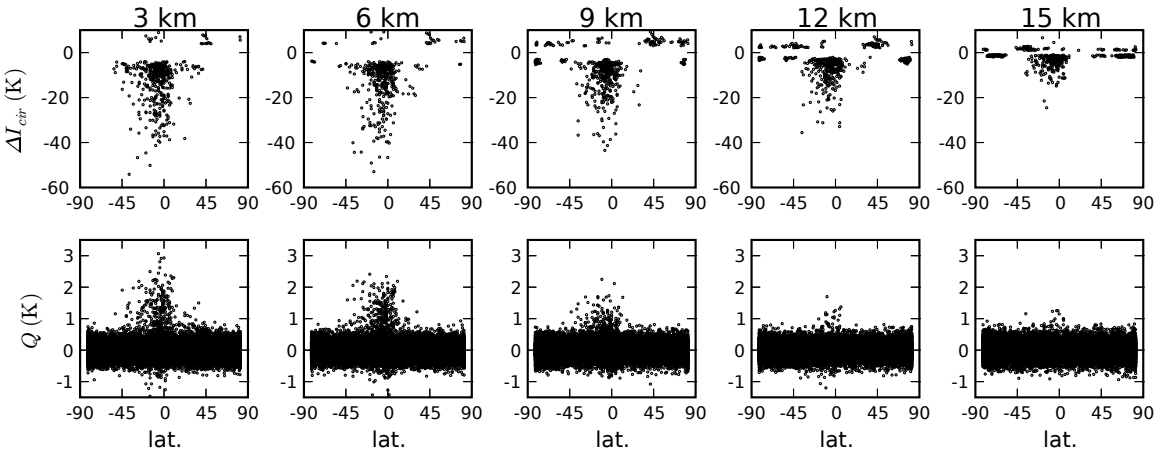

Figure 2. Cloud induced radiance, ΔI_{cir}, and polarization difference, Q, for January 3 - 8, 2005.